Lagrangian Formulation of a Linear Microstrip Resonator: Theory and Experiment

H. How, A. Widom, and C. Vittoria, *Fellow, IEEE*

***Abstract*—The electromagnetic scattering properties of a linear microstrip resonator are formulated utilizing a Lagrangian approach. The resonator design includes a center microstrip separated from the source and output loads by dielectric gaps. The gaps of the resonator are represented by capacitively coupled π-networks, whose capacitance values are fitted by experimental data. Calculated and measured reflection coefficients of linear microstrip resonators are compared and general agreements are found between theory and experiments.**

I. Introduction

TRADITIONALLY, the electromagnetic scattering data of a linear microstrip resonator is analyzed in terms of lumped RCL circuits. Each resonant mode is associated with a specific combination of RCL values. The coupling to the microwave source is represented by a coupling coefficient κ. κ is determined from analysis of measured line shapes of the resonant modes and intrinsic quality factor of the modes, Q_{in}. Specifically, Q_{in} is related to the measured quality factor Q_L by the following

$$Q_{\text{in}} = (1+\kappa)Q_L. \tag{1}$$

The above analysis was introduced by Ginston in 1957 [1]. It is clear in this analysis that the lumped circuit parameters associated with each resonant mode are not related to each other. Knowledge of the lumped RCL parameters of one mode is insufficient in predicting the parameters of other modes. Furthermore, the measured electromagnetic parameters, Q_{in} and κ, cannot be directly related to the circuit design parameters of a microstrip resonator, say, the dielectric loss, the conductor loss, and the gap separation.

In this analysis, we are proposing a new analysis in which one and only one set of parameters (C_1 and C_2) are introduced in the model to represent the electromagnetic scattering properties of the resonator at all frequencies or resonant modes. This is done by utilizing a Lagrangian approach, where the transmission line and the two gaps are formulated together as one system and in terms of the physical parameters of the microstrip line resonator. It is generally recognized that the Lagrangian approach provides the most convenient way of formulating the couplings between dynamical systems. Examples of coupled lumped electrical circuits, described in terms of Lagrangians, can be found in [2]. In this paper, we first formulate the Lagrangian of a microstrip transmission line in which a wave of the fundamental TEM mode of propagation is derived. While a gap in a microstrip line is modeled in terms of a capacitive π network, the Lagrangian is formulated in the discrete limit such that the equations of motion transform into two boundary conditions, relating the waves on the two sides of the gap in terms of two lumped capacitors. The effective capacitors expressed in the boundary conditions are actually the capacitances experienced by the even and odd excitation modes of the system, respectively. The calculations therefore take into account the characteristic impedance, effective dielectric constant, conductivity of the metal strip and the ground plane, and dielectric loss tangent of the dielectric material. In addition, the two capacitor values representing the gaps are included in a consistent manner with the above parameters by the application of the Lagrangian formulation. Reflection coefficients are calculated from our model and their predictions agree very well with the measurements.

Manuscript received April 5, 1990; revised November 20, 1990.
The authors are with the Department of Electrical and Computer Engineering, Northeastern University, Boston, MA 02115.
IEEE Log Number 9042505.

II. Theoretical Formulations

Fig. 1(a) shows the construction of a microstrip line where w, t, h, and ϵ_r are, respectively, the width, the thickness of the metal strip, the thickness, and the relative dielectric constant of the dielectric substrate. In the discrete limit, a (lossless) microstrip line is represented by distributed elements as shown in Fig. 1(b), where ϵ, μ, b, and $\dot{Q}_1$ are, respectively, capacitance per unit length, inductance per unit length of the transmission line, the length increment of the line, and the current flowing through the ith inductor of the line. The Lagrangian of the transmission line (of infinite length) is, therefore,

$$L = \sum_{i=-\infty}^{\infty} \left[\frac{\mu b}{2} \dot{Q}_i^2 - \frac{1}{2\epsilon b} (Q_{i+1} - Q_i)^2 \right].$$

In the continuum limit, L becomes

$$L = \int_{-\infty}^{\infty} dx \left[\frac{\mu}{2} \left(\frac{\partial Q}{\partial t} \right)^2 - \frac{1}{2\epsilon} \left(\frac{\partial Q}{\partial x} \right)^2 \right]. \tag{2}$$

The Lagrangian equation of motion is

$$\frac{\delta L}{\delta Q} - \frac{\partial}{\partial x} \left[\frac{\delta L}{\delta(\partial Q/\partial x)} \right] - \frac{\partial}{\partial t} \left[\frac{\delta L}{\delta(\partial Q/\partial t)} \right] = 0 \tag{3}$$

where $\delta L/\delta Q$ denotes functional derivative of L with respect to Q, etc. When (2) is substituted into (3), one obtains

$$\frac{\partial^2 Q}{\partial x^2} - \frac{1}{v^2} \frac{\partial^2 Q}{\partial t^2} = 0 \tag{4}$$

which is the wave equation of the TEM mode of propagation. The electromagnetic waves travel with a velocity v

0018-9480/91/0400-0660$01.00

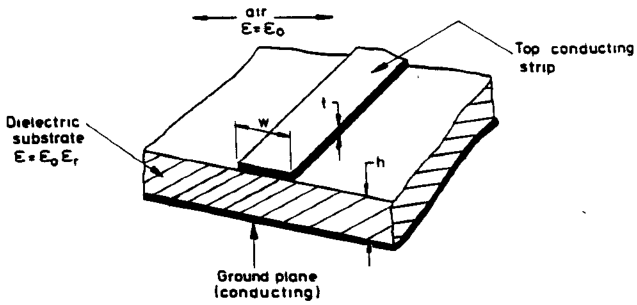

(a)

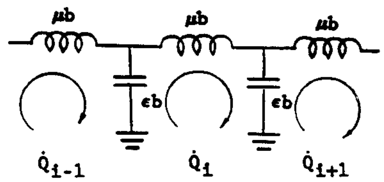

(b)

Fig. 1. (a) Microstrip line configuration. (b) Microstrip line represented by distributed capacitors and inductors.

given by

$$v = 1/\sqrt{\epsilon\mu}$$

where

$$\epsilon = \epsilon_{re}\epsilon_0$$

$$\mu = \mu_{re}\mu_0$$

and ϵ_0 and μ_0 are permittivity and permeability of free space, respectively. The relative permittivity and permeability of the line, ϵ_{re} and μ_{re}, become complex numbers if the line is lossy, and, for a narrow line $h > 0.8w$, ϵ_{re} and μ_{re} take the forms [3]

$$\epsilon_{re} = \epsilon' - i\epsilon'' \quad (5a)$$

$$\mu_{re} = \mu' - i\mu''. \quad (5b)$$

Here

$$\epsilon' = 0.475\epsilon_r + 0.67 \quad (6a)$$

$$\epsilon'' = \epsilon' F_\epsilon \tan\delta \quad (6b)$$

$$\mu' = 1 \quad (6c)$$

$$\mu'' = 2\alpha_c Z_0/\omega. \quad (6d)$$

ω is the angular frequency, ϵ_r is the relative dielectric constant of the dielectric substrate, $\tan\delta$ is the loss tangent of the substrate, α_c is the conductor attenuation constant, F_ϵ is the filling factor of the substrate material given by

$$F_\epsilon = 0.5\left[1 + (1 + 10h/w)^{-1/2}\right] \quad (6e)$$

and Z_0 is the characteristic impedance of the line. $\alpha_c Z_0$ can be derived from the following equation [3]:

$$\frac{\alpha_c Z_0 h}{R_s} = \frac{8.68}{2\pi}\left[1 - \left(\frac{w'}{4h}\right)\right]\left[1 + \frac{h}{w'} + \frac{h}{\pi w'}\left(\ln\frac{4\pi w}{t} + \frac{t}{w}\right)\right]. \quad (7)$$

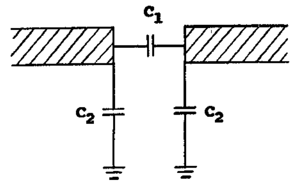

(a)

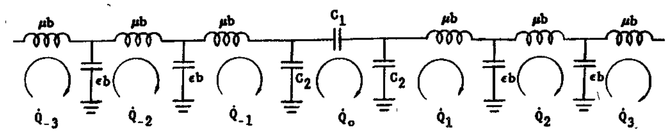

(b)

Fig. 2. (a) Capacitive π-network model of a microstrip gap. (b) Microstrip lines and gap represented in the discrete limit by capacitors and inductors.

In (7),

$$w' = w + \Delta w$$

$$\Delta w = \frac{t}{\pi}\left(\ln\frac{2h}{t} + 1\right)$$

and the surface impedance R_s is defined by

$$R_s = \sqrt{\frac{\omega\mu_0}{2\sigma}}$$

with σ being the conductivity of the metal strip and the ground plane.

When a gap is introduced in a microstrip line, as shown in Fig. 2(a), two lumped capacitors forming a π-network can be used to model the gap [4]. Capacitor C_1 describes the coupling of the excess charges accumulated at the two ends of the lines and capacitors C_2 correspond to the coupling between the strip excess charges and the image charges induced in the ground plane. As shown in Fig. 2(b), the Lagrangian of the system, two semi-infinite microstrip lines and a gap, can be described in the discrete limit as

$$L = \frac{\mu b}{2}\sum_{n=1}^{\infty}\left(\dot{Q}_n^2 + \dot{Q}_{-n}^2\right) - \frac{1}{2\epsilon b}\sum_{n=1}^{\infty}\left[(Q_{n+1} - Q_n)^2 + (Q_{-n-1} - Q_{-n})^2\right] - \frac{Q_0^2}{2Q_1} - \frac{1}{2C_2}\left[(Q_1 - Q_0)^2 + (Q_{-1} - Q_0)^2\right]. \quad (8)$$

Substituted into the Lagrangian equation

$$\frac{\partial L}{\partial Q_n} - \frac{\partial}{\partial x}\left[\frac{\partial L}{\partial(\partial Q_n/\partial x)}\right] - \frac{\partial}{\partial t}\left[\frac{\partial L}{\partial(\partial Q_n/\partial t)}\right] = 0 \quad (9)$$

one obtains

$$-\mu b\frac{d^2 Q_n}{dt^2} - \frac{1}{\epsilon b}(2Q_n - Q_{n+1} - Q_{n-1}) = 0, \quad \text{for } |n| > 1 \quad (10a)$$

$$-\mu b\frac{d^2 Q_{+1}}{dt^2} - \frac{1}{\epsilon b}(Q_{\pm 1} - Q_{\pm 2}) - \frac{1}{C_2}(Q_{\pm 1} - Q_0) = 0, \quad \text{for } n = \pm 1 \quad (10b)$$

$$Q_0 = \frac{C_1}{2C_1 + C_2}(Q_1 + Q_{-1}), \quad \text{for } n = 0. \quad (10c)$$

In the continuum limit, (10a) and (10b) become

$$\frac{\partial^2 Q}{\partial t^2} - \frac{1}{\epsilon\mu}\frac{\partial^2 Q}{\partial t^2} = 0, \qquad \text{for } x \neq 0 \tag{11}$$

$$\left.\frac{\partial Q}{\partial x}\right|_{x=0^+} = AQ|_{x=0^+} - BQ|_{x=0^-} \tag{12a}$$

$$\left.\frac{\partial Q}{\partial x}\right|_{x=0^-} = BQ|_{x=0^+} - AQ|_{x=0^-} \tag{12b}$$

where constants A and B are defined as

$$A = \frac{\epsilon}{2}\left(\frac{1}{C_2} + \frac{1}{2C_1 + C_2}\right) \tag{13a}$$

$$B = \frac{\epsilon}{2}\left(\frac{1}{C_2} - \frac{1}{2C_1 + C_2}\right) \tag{13b}$$

and (10c) has been used in deriving (12a) and (12b). Equation (11) is the same wave equation as derived in (4), and (12a) and (12b) turn out to be boundary conditions associated with the gap located at $x = 0$. Note that A and B are defined in terms of two capacitances, $2C_2$ and $2C_1 + C_2$, which are actually the effective capacitances associated with the even and odd mode excitations of the system containing the gap and the two microstrip lines, respectively.

Consider a microstrip linear resonator bounded by two identical gaps located at $x = 0$ and $x = a$ and fed by two semi-infinite microstrip lines called launcher (detector) lines. The launcher lines are considered to be lossless in order to make the boundary conditions at $x = \pm\infty$ simple. The wave propagating in the launcher lines satisfies (11), except ϵ and μ are replaced by $\epsilon'\epsilon_0$ and μ_0, respectively. Assume the wave has the following dependence:

$$Q = u(x)\exp(-i\omega t)$$

and $u(x)$ takes the following form:

$$\begin{aligned} u(x) &= \exp(ix/x_0) + \rho\exp(-ix/x_0) && \text{for } x < 0 \\ &= \alpha\cos(x/x_1) + \beta\sin(x/x_1) && \text{for } 0 < x < a \\ &= \tau\exp(ix/x_0), && \text{for } x > a, \end{aligned} \tag{14}$$

where x_0 and x_1 are defined as

$$x_0 = \frac{1}{\omega}\sqrt{\frac{1}{\epsilon'\epsilon_0\mu_0}}$$

$$x_1 = \frac{1}{\omega}\sqrt{\frac{1}{\epsilon\mu}}.$$

From (12a) and (12b), the boundary conditions at $x = 0$ and $x = a$ require

$$\beta/x_1 = A\alpha - B(1+\rho) \tag{15a}$$

$$i(1-\rho)/x_0 = B\alpha - A(1+\rho) \tag{15b}$$

$$i\tau e/x_0 = A\tau e - B(\alpha c + \beta s) \tag{15c}$$

$$(-\alpha s + \beta c) = B\tau e - A(\alpha c + \beta s) \tag{15d}$$

where e, c, and s are defined as

$$e = \exp(ia/x_0)$$

$$c = \cos(a/x_1)$$

$$s = \sin(a/x_1).$$

Therefore, the four unknowns ρ, α, β, and τ can be solved through (15a)–(15d). The reflection coefficient ρ is found to be

$$\rho = \frac{w-1}{w+1} \tag{16}$$

where

$$w = \frac{i}{A^2 - B^2}\left\{-\frac{A}{a} + \frac{B^2}{a^2(A^2-B^2)\{\eta t + (t^2+1)/[aA - t/\eta - a^2B^2/(aA+i)]\} + A}\right\}$$

$$t = \tan(a/x_1)$$

$$\eta = x_1/x_0.$$

TABLE I
INFORMATION ABOUT RESONATORS #1 TO #5

Microstrip Linear Resonators	#1	#2	#3	#4	#5
Gap (cm)	0.105	0.085	0.065	0.045	0.025
Linear Dimension (cm)	0.79	0.83	0.87	0.91	0.95
Resonance Observed?	No	(very small)	Yes	Yes	Yes

The last item that needs to be clarified is the resonator length. Due to the fringe fields around the open ends of the resonator, the effective length of the resonator, a, is larger than its physical length, a_0. From [4], we have

$$a = a_0 + 2\delta a$$

where

$$\delta a = NZ_0(C_1 + C_2)\Big/\sqrt{\epsilon'\epsilon_0\mu_0} \tag{17}$$

and N is a constant of magnitude unity. As shown in the following section, in order to best describe the experimental data N is found to have value 0.307.

III. Experimental Results

Microstrip resonators were fabricated by us utilizing RT/duroid 6010 laminates which have the following nominal values: $h = 0.635$ mm, $t = 15$ μm, $\epsilon_r = 10.2 \sim 10.5$, $\tan\delta = 0.0023$, and $\sigma = 5.8\times10^7$ mho/m. The dielectric constant of the substrate material was found to be frequency dependent

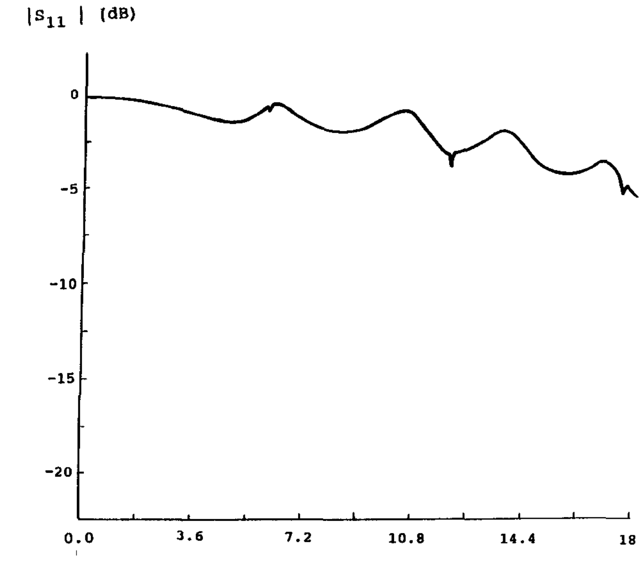

Fig. 3. Experimental reflection data for resonator #3.

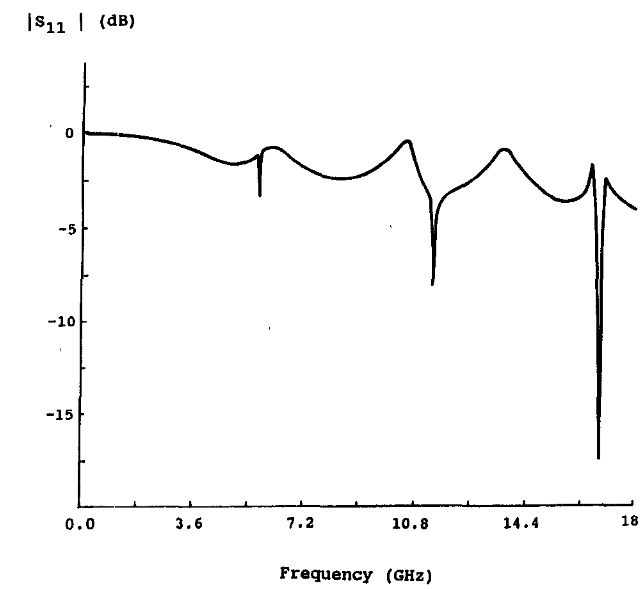

Fig. 4. Experimental reflection data for resonator #4.

of the following form:

$$\epsilon_r = 10.2 + 0.0147 \cdot f \tag{18}$$

and f is in GHz. The constant ϵ_r was determined from fitting calculated and measured values of reflection coefficients from 0.1 to 18 GHz. Furthermore, all the microstrip lines were designed of width $w = 0.65$ mm in order to have the characteristic impedance of the lines, Z_0, equal to 50 Ω.

As outlined in Table I, five resonators were fabricated with gaps ranging from 0.105 to 0.025 cm and linear dimension, a_0, ranging from 0.79 to 0.95 cm. The total length of all the circuits, including the resonator, the two gaps, and the two launcher (detector) lines, was 3 cm. The circuits were tested utilizing a network analyzer, HP8510B. Resonators #1 and #2 showed very little resonant structure, since the coupling is small between launcher and resonator for large

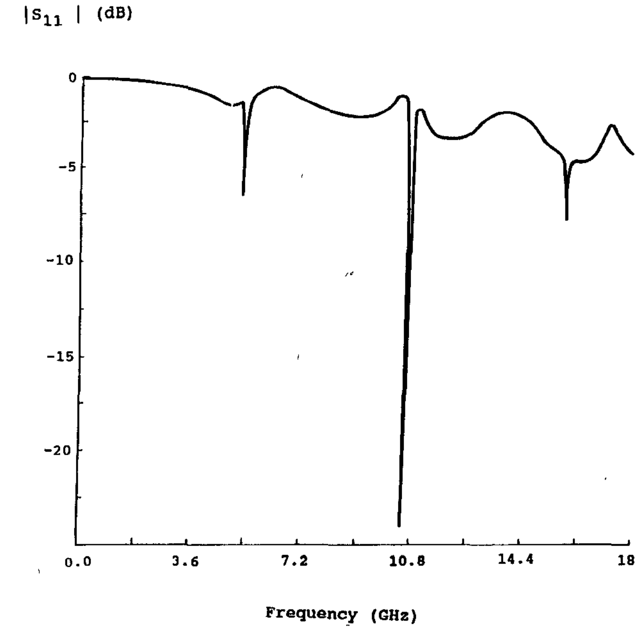

Fig. 5. Experimental reflection data for resonator #5.

gaps. Therefore, only resonators #3, #4, and #5 will be discussed in this paper.

Figs. 3–5 exhibit measured S_{11} data on resonators #3 to #5, respectively. The frequency ranged from 0.1 to 18 GHz, and 801 data points were taken during the frequency sweep. For each resonator, three resonant peaks were observed as S_{11} was measured from 0.1 to 18 GHz. The S_{11} data were composed of background and resonant signals. The background signal arises from the very low Q electromagnetic standing mode resonances of the electromagnetic waves within the launcher lines. We were able to separate the background from resonant signal by fabricating microstrip lines without the central resonator, a circuit containing only the open structure of the launcher lines and detector lines.

Data on the nine resonant peaks of the three resonators are tabulated in Table II. The data include resonant frequencies, intensities, and quality factors of each measured resonant mode (numbered from 1 to 3 for resonators #3 to #5). The effective increment of the resonator length, δa, can also be calculated from the measured reflection data via the following equation:

$$2\delta a = \frac{1}{2}\frac{cn}{f_{\mathrm{res}}\sqrt{\epsilon'}} - a_0 \tag{19}$$

where c is the velocity of light in vacuum, and f_{res} and n are the resonant frequency and the order of the resonant peak, respectively. δa values calculated by (19) are also included in Table II.

Theoretical predictions of the reflection data of the resonators #3–#5 can be calculated via formulas outlined in the previous section, provided that the two lumped capacitor values C_1 and C_2 are known. In this analysis, C_1 and C_2 are obtained via data fitting: we require the frequency and the intensity of the fundamental mode of the resonators to be the same for both the theory and the measurements. This determines uniquely C_1 and C_2 and their values are tabulated in Table II. Using these C_1 and C_2 values, the associated reflection characteristics of resonators #3–#5 can be

TABLE II
COMPARISON BETWEEN THEORY AND EXPERIMENT FOR RESONATORS #3 TO #5

Resonator	#3			#4			#5			
Peak No.	1	2	3	1	2	3	1	2	3	Method
Resonant	6.03	11.87	17.44	5.83	11.42	16.83	5.51	10.84	15.96	Meas.
Freq. (GHz)	6.03	11.87	17.49	5.83	11.42	16.81	5.51	10.84	16.03	Calc.
Peak Height	−0.50	−0.70	−0.86	−2.15	−4.37	−20.7	−4.45	−23.8	−3.82	Meas.
(dB)	−0.50	−1.07	−1.36	−2.15	−4.07	−5.24	−4.45	−7.75	−9.21	Calc.
Q Value	108	152	195	87	102	125	62	65	75	Meas.
	108	177	156	130	113	60	41	33	28	Calc.
δa (mm)	0.91	0.96	1.02	0.89	0.96	1.03	1.01	1.06	1.11	Meas.
	0.97	0.96	0.96	0.94	0.93	0.93	1.09	1.08	1.08	Calc.
C_1 (pF)		0.007			0.013			0.024		Cited
		0.048			0.107			0.180		Calc.
C_2 (pF)		0.031			0.025			0.017		Cited
		0.451			0.376			0.372		Calc.

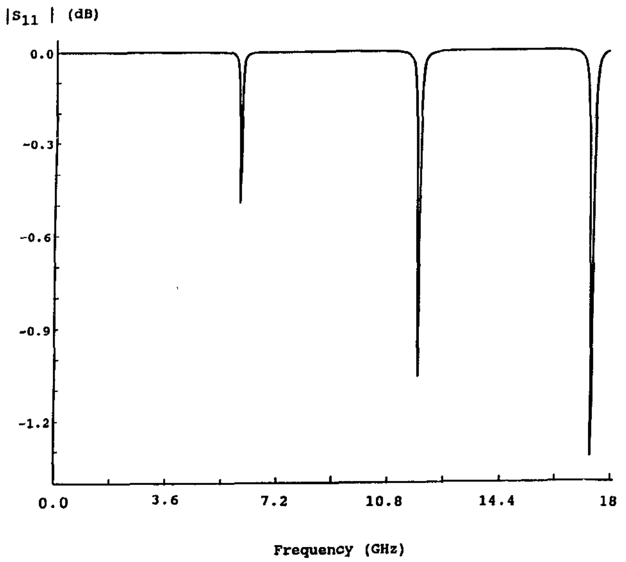

Fig. 6. Theoretical reflection data for resonator #3.

calculated and the result for that of resonator #3 is shown in Fig. 6. Information about the resonant modes of the resonators predicted by the theory are summarized in Table II, including the resonant frequencies, the intensity, and the quality factors. δa values calculated via (17) are also tabulated in Table II, where the constant N is chosen to be 0.307 in order to best fit the experimental data.

Field calculations (solution of singular integral equations) concerning excess charge distributions near gaps in microstrip transmission lines can provide estimates [5] about the magnitudes of C_1 and C_2. For resonators #3–#5, the associated C_1 and C_2 values calculated in this way and cited from [5] are listed in Table II. We note that the C_1 values found by us are several times larger and C_2 values one order of magnitude larger than the values derived by pure-field considerations [5]. However, the trends of variations of C_1 and C_2 with gap separations are the same as those found in [5]: C_2 scales as the width of the gap whereas C_1 as the inverse.

Careful examination of Table II reveals that our theory predicts very well the resonant frequencies and δa values of the resonators. In addition, good agreement was found between theory and experiments for the peak height signal and Q values of the resonators. However, we should point out two cases in which the agreement between calculated and measured resonant intensities was poor: the third peak of resonator #4 and the second peak of resonator #5. We attribute this discrepancy to the incomplete treatment of our theoretical model. In the theory, we have treated the launcher (detector) lines to be semi-infinitely long. In reality, the launcher lines are only of finite lengths and hence provide an oscillatory background structure for the S_{11} measurements. Extraordinary interaction between the central microstrip resonator and the launcher lines occurs, if the resonant frequencies of launcher lines and resonator coincide, i.e., the resonant peaks are situated at the crests of the background oscillations. This statement can be qualitatively proved by applying the Fermi–Golden rule [6] to microwave circuits. When a photon is excited in the central resonator, the lifetime of the photon, i.e., the Q of the resonator, depends inversely on the transition rate of the photon from its initial state of the resonator to a final state on the launcher line. The photon transition rate is proportional to the state density of the final states. The density of states of the photon modes on the launcher lines has much lower values for frequencies located at the background oscillation crests than when they are located elsewhere. Therefore, the photon modes are much more isolated when the frequencies are located at the crests and so the resonant peaks intensify tremendously in these situations. A complete treatment of this problem includes modeling of the two launcher lines of finite length, superimposed by the boundary conditions at the other ends of the launcher lines where the effects of coaxial-line to microstrip-line adaptors have to be considered.

IV. CONCLUSIONS

We have formulated the Lagrangian of a linear microstrip resonator from which resonant behaviors of all modes can be described in a single model. With this approach, there is no need to introduce any artificial parameter in describing the data, such as the coupling coefficient of the lumped RCL circuit in Ginston's model [1]. The theory, in general, predicts the following: as the order of the resonant mode increases, the peak intensity increases and the Q decreases; when the gap separation increases, C_1 decreases, C_2 increases, and δa decreases. These general conclusions compare reasonably well with our experimental findings. Our theoretical model can be further refined if the launcher line is assumed to be finite rather than semi-infinite. Nevertheless, the Lagrangian formulation lends readily itself to transmission line perturbations discussed here.

References

[1] E. L. Ginzton, *Microwave Measurements*. New York: McGraw-Hill, 1957, p. 391.

[2] L. D. Landau, E. M. Lifshitz, and L. P. Pitaevskii, *Electrodynamics of Continuous Media*. New York: Pergamon Press, 1984, pp. 215–217.

[3] R. K. Hoffman, *Handbook of Microwave Integrated Circuits*. Norwood, MA: Artech House, 1987, pp. 148 and 194.

[4] T. C. Edwards, *Foundations for Microstrip Circuit Design*. New York: Wiley, 1981, p. 105.

[5] P. Benedek and P. Silvester, "Equivalent capacitances for microstrip gaps and steps," *IEEE Trans. Microwave Theory Tech.*, vol. MTT-20, pp. 729–733, 1972.

[6] L. I. Schiff, *Quantum Mechanics*. McGraw-Hill, 1955, p. 199.

H. How, photograph and biography not available at the time of publication.

A. Widom, photograph and biography not available at the time of publication.

C. Vittoria (S'62–M'63–M'80–SM'83–F'90), photograph and biography not available at the time of publication.